

Adsorptive removal of Cr(VI) from aqueous solution using rice husk and rice husk ash

Gopal Chandra Ghosh*, Samina Zaman, Tapos Kumar Chakraborty

Department of Environmental Science and Technology, Jessore University of Science and Technology, Jessore 7408, Bangladesh, Tel. +88 01760115579; Fax: +88 421 61199; emails: gopales8@hotmail.com (G.C. Ghosh), saminazaman25@gmail.com (S. Zaman), taposchakraborty@rocketmail.com (T.K. Chakraborty)

Received 18 October 2017; Accepted 24 July 2018

ABSTRACT

This study investigated the removal of hexavalent chromium (Cr(VI)) by rice husk and rice husk ash from aqueous solution using different doses of adsorbent (5–25 g/L), initial Cr(VI) concentration (5–100 mg/L), pH (2–8), and contact time (5–150 min). Maximum Cr(VI) removal was observed at pH 2. The results revealed that Cr(VI) removal efficiency increases with an increase of the adsorbent dose, but the removal efficiency decreases with an increase of initial Cr(VI) concentration, while keeping all the other parameters constant. The efficiencies of rice husk and rice husk ash for Cr(VI) removal were 94.0% and 88.4%, respectively, from solutions containing 5.0 mg/L of Cr(VI) at a pH of 2 and adsorbent concentration of 20 g/L after 150 min of equilibration. The pseudo-second-order model was superior to pseudo-first-order model in adsorption and was controlled by chemisorptions and intraparticle diffusion process. Among Freundlich and Langmuir isotherms, the latter had a better fit with the experimental data. The maximum Langmuir adsorption capacities were 3.78 and 2.27 mg/g for rice husk and rice husk ash, respectively. Overall, the results suggest that both rice husk and rice husk ash are efficient low- or no-cost adsorbent, useful for the removal of Cr(VI) from aqueous solution.

Keywords: Adsorption; Rice husk; Rice husk ash; Chromium; Isotherm; Kinetic

1. Introduction

Water pollution by heavy metal is one of the most important environmental quality and human health problems today [1]. Among heavy metals, chromium is one of the most hazardous heavy metals, which is present in the effluent from industries that use chromium, such as industries involved in electroplating, leather tanning, textile production, and the manufacturing of chromium-based product [2]. In aqueous systems, chromium exists primarily in the trivalent Cr(III) and hexavalent Cr(VI) oxidation states which have very different physicochemical properties and effects on living organisms [3]. Cr(VI) is about 300 times more toxic than Cr(III) and due to the fact that it has high water solubility,

it can transport long distance, and highly bioavailable [4]. Therefore, it is necessary to substantially remove Cr(VI) from the wastewater before being discharged into the aquatic system. A number of treatment methods for the removal of heavy metal from aqueous solutions have been reported including adsorption [3,5], chemical and electrochemical precipitation [6,7], ion exchange [8], membrane filtration [9,10], and photolysis [11]. The most common method used for removal of Cr(VI) is reduction-precipitation. The disadvantages of this treatment are: require a large amount of chemicals, generate volumetric sludge, and cost more for the treatment. Among heavy metal removing technologies, adsorption has become by far the most versatile and widely used technology, and activated carbon is the most commonly used sorbent, but it is relatively expensive. Furthermore, commercial activated carbon shows low Cr(VI) adsorption capacity [12]. The use of algae [13], bacteria [14], fungi [15], and different plants

* Corresponding author.

[16,17] as adsorbent has been reported, but their practical application may not be suitable due to their relatively poor natural abundance and cost of production [18].

Adsorption onto agricultural waste is a low-cost treatment technique for the removal of contaminants, including heavy metals, from water and wastewater. An agro-industrial residue that is widely accessible in most of the rice-producing countries is rice husk (RH). The RH is the outermost layer of the paddy grain that is separated from the rice grains during the milling process. RH is largely considered a waste product that is often burned and produces rice husk ash (RHA). Around 20% of paddy weight is husk and rice production in Asia produces about million tons of husks annually [19]. RH mainly consists of crude protein (3%), ash (including silica 17%), lignin (20%), hemicellulose (25%), and cellulose (35%) renders it suitable for metallic cations fixation [20]. Several studies have reported the use of RH as an adsorbent for the removal of metals including chromium [20–22]. Srivastava et al. [23] reported the efficacy of RHA as an adsorbent for the individual removal of Cd(II), Ni(II), and Zn(II) from synthetic solution. The use of RHA as adsorbent for Cr(VI) removal is still hindered by lack of information.

The RH and RHA are available in large quantity in Bangladesh and many other rice producing countries at low-or no-cost. Additionally, the use of agro-industrial residues as adsorbents holds promise as an environment-friendly way to substitute or supplement commercially available adsorbents, particularly in areas without access to centralized wastewater treatment facilities. Therefore, the objective of this study is to investigate the applicability of RH and RHA in their natural form to remove Cr(VI) from aqueous solution. The effects of pH, initial Cr(VI) concentration, contact time, and adsorbents dose have been investigated. The kinetics and adsorption isotherms were also evaluated. Afterwards, the efficiency of RH and RHA were investigated in the removal of Cr(VI) from tannery wastewater. The information obtained may be useful for modeling and designing the adsorption processes.

2. Materials and methods

2.1. Preparation of adsorbents and characterization

RH and RHA were collected from a rice processing mill in Jessore, Bangladesh. In the rice mill, RH is used as fuel to produce steam. The impurities in the materials were separated manually and washed thoroughly with double distilled water. The soluble colored components were then removed by washing repeatedly with hot double distilled water (70°C), filtered, and dried at 105°C in hot air oven for 48 h. The materials were stored in airtight borosilicate glass bottles and used for experiments as needed. IR spectra of fresh and Cr(VI)-loaded RH and RHA were recorded in a FTIR-8400S (Fourier transform infrared spectroscopy), Shimadzu, Japan. The surface morphology of fresh and Cr(VI)-loaded RH and RHA were observed with a scanning electron microscope (FESEM: JEOL JSM 7600F) equipped with energy dispersive X-ray spectroscopy (EDS).

2.2. Preparation and analysis of test water

All the chemicals used were ACS reagent-grade and double distilled water was used for preparation of the solution

throughout the experiments. Aqueous stock solution of Cr(VI) was prepared by dissolving 1 g of potassium chromate in 1 L double distilled water. pH of the solutions was measured using a pH meter (model pH56, Milwaukee Instruments, Inc., USA). The analysis of Cr(VI) was carried out using a spectrophotometer (HACH DR 2700; method 8023) according to the 1,5-diphenylcarbohydrazide method using a single dry powder formulation called ChromaVer® 3 chromium reagent for Cr(VI). The electrical conductivity (EC), total dissolved solids (TDS), and salinity were measured using a portable conductivity/TDS meter (sensION®EC5, HACH). The applicability of RH and RHA in the removal of Cr(VI) from wastewater was evaluated using wastewater sample collected from a tannery located in Hazaribagh Tannery Area, Dhaka, Bangladesh.

2.3. Batch adsorption experiments

The adsorption batch experiments were carried out in 500 mL beakers with 200 mL working volume solution with adsorbent. In the tests, 200 mL of a known Cr(VI) solution (prepared from the dilution of 1 g/L stock solutions) was poured into each beaker, and the pH was adjusted (using 0.1 N HCl/0.1 N NaOH), a given mass of either RH or RHA was added to the solution and stirring speed was kept at 200 rpm for an equilibrium contact time of 150 min. The effects of pH 2–8, adsorbent dose (5–25 g/L), and initial Cr(VI) concentration (5–100 mg/L) on Cr(VI) adsorption were studied, while all the other parameters were kept constant. Upon completion, a sample of the suspension was removed from the beaker and filtered through a fiberglass filter (0.2 m pore size) to remove adsorbent particles. The filtrate was diluted and analyzed for residual Cr(VI). All batch experiments were conducted in a Jar-test instrument (JLT4, VELP Scientific, Italy) and performed in duplicate. Under the experimental conditions, the amount of Cr(VI) adsorbed at equilibrium was calculated using Eq. (1).

$$q_e = \frac{(C_o - C_e)V}{m} \quad (1)$$

where C_o and C_e are the initial and at equilibrium Cr(VI) concentrations in mg/L, respectively. q_e is the equilibrium Cr(VI) uptake in mg/g. V is the volume of solution (L) and m is the mass of adsorbent (g).

The percentage removal of Cr(VI) was calculated using Eq. (2).

$$R(\%) = \frac{(C_o - C_e)}{C_o} \times 100 \quad (2)$$

2.4. Isotherm experiments

In order to carry out the adsorption isotherm experiments, Cr(VI) adsorption on RH and RHA were conducted at the optimum conditions using a contact time of 150 min at pH 2 with each adsorbent dose of 5, 10, 15, 20, and 25 g/L and a fixed Cr(VI) concentration of 50 mg/L. The capacity of an adsorbent can be described by equilibrium adsorption isotherms which express the affinity and surface properties of the adsorbent. In this study, equilibrium adsorption was

modeled using the Langmuir and the Freundlich isotherms because of their ease of interpretation. The Langmuir isotherm has been successfully applied to the adsorption processes of heavy metal ions. The basic assumption of the Langmuir model is that sorption takes place on a homogeneous surface by monolayer sorption without interaction between adsorbed molecules. The linear form of the Langmuir equation after rearrangement is presented in Eq. (3) as follows:

$$\frac{C_e}{q_e} = \frac{1}{q_{\max} b} + \frac{C_e}{q_{\max}} \quad (3)$$

where C_e is the equilibrium concentration of remaining Cr(VI) in the solution (mg/L), q_e is the amount of Cr(VI) adsorbed per mass unit of adsorbent at equilibrium (mg/g), q_{\max} is the amount of Cr(VI) at complete monolayer coverage (mg/g), and b (L/mg) is Langmuir constant related to adsorption capacity and rate of adsorption, respectively. The Langmuir parameters can be determined from the slope and intercept when plotting C_e/q_e versus C_e .

The essential feature of the Langmuir isotherm can be expressed in terms of dimensionless constant separation factor (R_L) that is used to predict whether an adsorption system is “favorable” or “unfavorable” [24]. The separation factor is defined in Eq. (4) as follows:

$$R_L = \frac{1}{1 + bC_0} \quad (4)$$

The adsorption process as a function of R_L may be described as $R_L > 1$, unfavorable; $R_L = 1$, linear; $0 < R_L < 1$, favorable; and $R_L = 0$, irreversible.

The empirical Freundlich model considers no surface saturation and can be represented in linear form in Eq. (5) as follows:

$$\log q_e = \log K_f + \frac{1}{n} \log C_e \quad (5)$$

where K_f and n are Freundlich constants indicating adsorption capacity and intensity, respectively. K_f and n can be determined from a linear plot of $\log q_e$ against $\log C_e$.

2.5. Kinetic experiments

Kinetic experiments were performed using beakers containing 200 mL of Cr(VI) solution at concentrations of 50 and 100 mg/L, and 20 g/L of either RH or RHA. In each test, 200 mL of Cr(VI) solution with the desired concentration was added to each flask and the pH was adjusted to 2. After the adjustments, 20 g of RH or RHA was added and the resultant suspension was stirred at 200 rpm at $25^\circ\text{C} \pm 2^\circ\text{C}$. Samples of 2 mL each were drawn from the solution mixture at time intervals of 5, 10, 15, 20, 30, 60, 90, 120, and 150 min and analyzed for kinetics study. In order to investigate the kinetics of biosorption, two kinetic models, Lagergren’s pseudo-first-order model [25] and Ho’s pseudo-second-order model [26] were employed. Lagergren first-order model can be represented in linear form in Eq. (6) as follows:

$$\log(q_e - q_t) = \log(q_e) - \frac{K_1}{2.303} t \quad (6)$$

where K_1 is the pseudo-first-order rate constant and q_t is the amount of Cr(VI) adsorbed (mg/g) at time t . The plot of $\log(q_e - q_t)$ against t should give a linear relationship from which K_1 and q_e can be determined from the slope and intercept of the plot, respectively. The pseudo-second-order model can be represented in linear form (with boundary conditions $t = 0$ to $t = t$ and $q_t = 0$ to $q_t = q_e$) in Eq. (7) as follows:

$$\frac{t}{q_t} = \frac{1}{k_2 q_e^2} + \frac{1}{q_e} t \quad (7)$$

where K_2 is the rate constant of pseudo-second-order adsorption (g/mg/min).

Replacing the term $K_2 q_e^2$ by h in Eq. (7) we have Eq. (8).

$$\frac{t}{q_t} = \frac{1}{h} + \frac{1}{q_e} t \quad (8)$$

where h is the initial adsorption rate (mg/g/min).

The Weber and Morris’s intraparticle diffusion kinetics model [27] consists of a simple model in which the rate of intraparticle diffusion can be obtained by linearization of the curve presented by Eq. (9). The applicability of this model indicates the presence of the intraparticle diffusion process.

$$q_t = K_w t^{0.5} + C \quad (9)$$

where C is the intercept and K_w is the intraparticle diffusion rate constant (mg/g/min^{0.5}) which can be evaluated from the slope of the linear plot of q_t versus $t^{0.5}$.

3. Results and discussion

3.1. Effect of pH on Cr(VI) removal

The effect of pH on chromium (concentration 5 mg/L) removal by RH and RHA were studied by varying the pH from 2 to 8 (Fig. 1). The pH of the solution has been identified as one of the most important variables governing Cr(VI) adsorption onto RH and RHA. As the pH of the solution

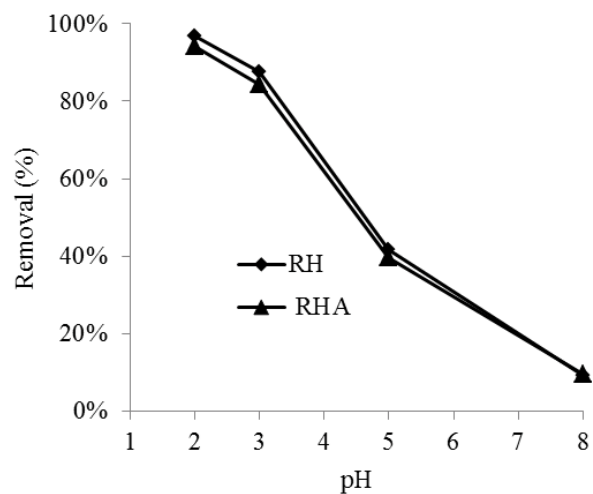


Fig. 1. Effect of pH on removal of Cr(VI) by RH and RHA.

was increased from 2 to 8, the adsorption of Cr(VI) onto RH and RHA was decreased. The average Cr(VI) removal by RH decreased from 96.0% to 9.2% when the pH of solution increased from 2 to 8. Similarly, increasing pH from 2 to 8, percent removal of Cr(VI) by RHA decreased from 94.2% to 9.6%. It was observed that the maximum adsorption was at pH 2. The pH-dependency of Cr(VI) removal by the adsorbents is a direct result of the dominant form of chromium present at different pHs. According to the solubility equilibrium of chromium, HCrO_4^- is the dominant species of Cr(VI) at a pH between 2 and 3 [28]. Increase in pH shifts concentration of HCrO_4^- to other forms, CrO_4^{2-} and $\text{Cr}_2\text{O}_7^{2-}$. So, the active form of Cr(VI) that can be easily adsorbed by RH and RHA was HCrO_4^- . This is due to the fact that the solution pH influences the chemical speciation of the metal ions as well as the ionization of the functional groups onto the adsorbents surfaces [29].

3.2. Effect of initial Cr(VI) concentration and contact time

The effect of initial Cr(VI) concentration and contact time on adsorption by the adsorbents at a constant dose of 20 mg/L is illustrated in Fig. 2. It can be seen that the percent removal, that is, percent adsorption, of Cr(VI) increases with an increase in contact time at each concentration and reach equilibrium at about 150 min and thereafter, it remains constant. Initially, there are many active sites onto the adsorbents and as time progressed, the adsorbate binds with the sites until every site becomes occupied and there is no further adsorption. However, Cr(VI) removal efficiency decreased with an increase of initial Cr(VI) concentration. For example, at each equilibrium time, Cr(VI) removal efficiency by RH and RHA decreased from 72% to 60% and 51% to 32%, respectively, with an increase in initial Cr(VI) concentration from 50 to 100 mg/L (Fig. 2). As the adsorbents have a limited number of binding sites at a constant dose which become saturated at certain concentration of adsorbate, more Cr(VI)

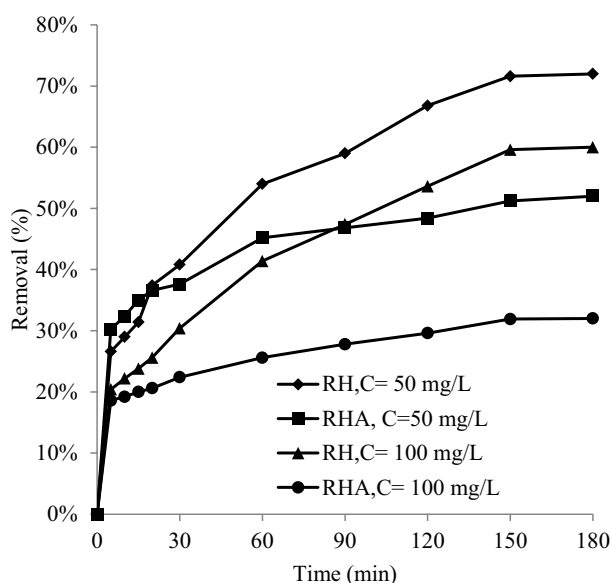


Fig. 2. Effect of initial Cr(VI) concentration and contact time on removal of Cr(VI) by RH and RHA.

remain unadsorbed in the solution due to the saturation of the binding sites, resulting in decreased removal efficiency at higher initial concentration of Cr(VI) [21,30]. Thus, the removal of Cr(VI) by adsorption onto RH and RHA depends on the initial concentration of Cr(VI) and contact time.

3.3. Effect of adsorbent dose on adsorption

The effect of adsorbent (RH and RHA) dose, ranging from 5 to 25 g/L, on the removal of Cr(VI) was evaluated at constant pH 2, contact time (150 min), stirring speed (200 rpm), and temperature ($25^\circ\text{C} \pm 2^\circ\text{C}$). Fig. 3 shows the average removal of Cr(VI) versus the adsorbent doses at concentration 5 and 50 mg/L, indicating the removal of Cr(VI) increased with increasing adsorbent dose. Moreover adsorption of Cr(VI) by RH has been found to be higher than RHA. Improve removal with increasing RH and RHA dose for each concentration of Cr(VI) can be attributed to increase in the ratio of adsorbent to adsorbate, which increase the surface area and the number of sites available for adsorption [21,23]. As shown in Fig. 3, the removal efficiencies of Cr(VI) is higher (60%–95.2% by RH and 47.6%–92% by RHA) at 5 mg/L concentration than 50 mg/L concentration (26.4%–77.2% by RH and 17.8%–67% by RHA) with various doses (5–25 g/L) of RH and RHA. Therefore, the optimum dose of RH and RHA depends directly on the concentration of Cr(VI); a higher Cr(VI) concentration requires a greater dose of RH and RHA. In contrast, adsorption capacity decreases with increasing adsorbent dose (Table 1), is mainly because of unsaturation of adsorption sites through the adsorption process. Adsorption capacity of RH and RHA were decreased from 2.64 to 1.54 and 1.78 to 1.34 mg/g, respectively, as the dose increased from 5.0 to 25.0 g/L at 50 mg/L of Cr(VI).

3.4. Modeling of adsorption isotherm

In this study, the Langmuir and Freundlich isotherm models were evaluated. They not only provide a general idea

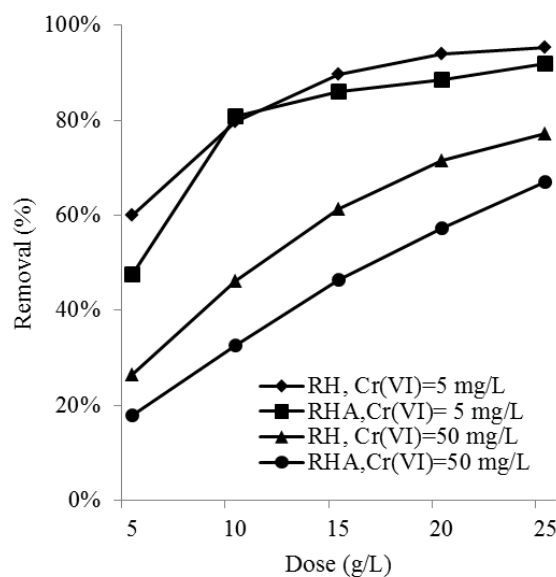


Fig. 3. Effect of RH and RHA dose on removal of Cr(VI).

Table 1
Adsorption capacity of RH and RHA at different adsorbent doses

Adsorbent dose (g/L)	RH (q_e , mg/g)	RHA (q_e , mg/g)
5	2.64	1.78
10	2.31	1.63
15	2.05	1.55
20	1.79	1.43
25	1.54	1.34

of the adsorbent effectiveness in removing the Cr(VI), but also indicate the maximum amount of Cr(VI) that will be adsorbed by the adsorbents [31]. The Langmuir and Freundlich isotherm plots are given in Figs. 4 and 5. The adsorption isotherm parameters calculated for biosorption of Cr(VI) are presented in Table 2. The results revealed that adsorption of Cr(VI) on RH and RHA fit better with the Langmuir model as compared with the Freundlich models. This result suggested that the adsorption of Cr(VI) occurred on a monolayer of the adsorbents surface. The maximum adsorption capacity of Cr(VI) onto RH and RHA, obtained from the fitted Langmuir model, was 3.78 and 2.27 mg/g, respectively (Table 2). The adsorption capacities for the RH and RHA indicate potential for the removal of Cr(VI) from aqueous solution, with the order RH > RHA. According to the data provided in Table 2, the value of the constant n in the Freundlich model is greater than 1, which confirms the suitability of both RH and RHA as adsorbent for Cr(VI) adsorption from aqueous solution. The R_L value calculated for RH and RHA from the Langmuir isotherm lies within 0 and 1, confirms the favorable adsorption of Cr(VI) in the adsorption process (Table 2).

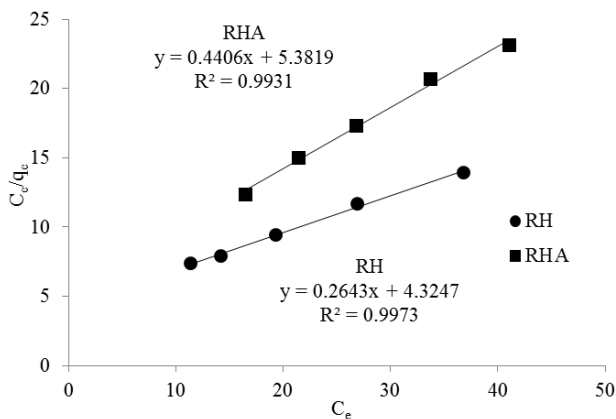


Fig. 4. Langmuir isotherm plot for adsorption of Cr(VI) on RH and RHA.

Table 2
Isotherm parameters for Cr(VI) adsorption on RH and RHA

Adsorbent	Langmuir isotherm				Freundlich isotherm		
	q_{max} (mg/g)	b (m/g)	R^2	R_L	K_f (mg/g)	n	R^2
RH	3.784	0.061	0.997	0.246	0.542	2.262	0.989
RHA	2.270	0.082	0.993	0.196	0.565	3.274	0.990

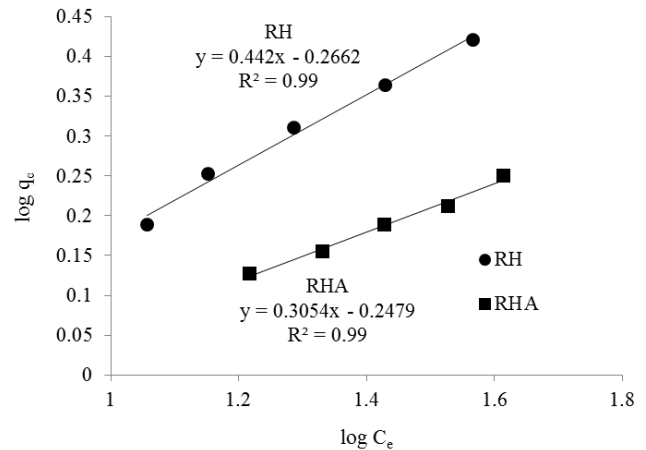


Fig. 5. Freundlich isotherm plot for adsorption of Cr(VI) onto RH and RHA.

3.5. Kinetic modeling

The kinetics informs the rate of adsorption of Cr(VI) onto the adsorbents and therefore is required for modeling and design of adsorption process. In order to clarify the adsorption process, the fitness of experimental data to pseudo-first-order and pseudo-second-order model was tested. Figs. 6 and 7 show the plot of pseudo-first-order and pseudo-second-order models for adsorption of the system, respectively. The kinetic information obtained from the models is summarized in Table 3, and it was found that the pseudo-second order model fits better than the pseudo-first-order model. Furthermore, the calculated adsorption capacity is close to the experimental adsorption capacity ($q_{e,exp}$) for pseudo-second-order model for both RH and RHA (Table 3). This indicates the sorption of Cr(VI) onto RH and RHA surface due to the chemisorption mechanism, including the sharing or exchanging of electrons between metal ion and adsorbent. The pseudo-second-order rate constant (K_2) was higher for 50 mg/L of Cr(VI) than 100 mg/L of Cr(VI) under similar experimental conditions. This result confirms that a rate enhancement due to mass transfer occurs with an increase in the concentration gradient [27]. The values in the Table 3 indicate that the initial rate of adsorption increases with increasing in initial concentration of Cr(VI), and initial adsorption rate of Cr(VI) by RHA is higher than RH at each concentration. As can be seen in Fig. 2, in the first minutes there is a relatively fast adsorption of Cr(VI), indicating the application of the adsorbents in the removal of Cr(VI).

The adsorbate transport from the liquid phase to the surface of the adsorbent occurs in several steps. The possibility

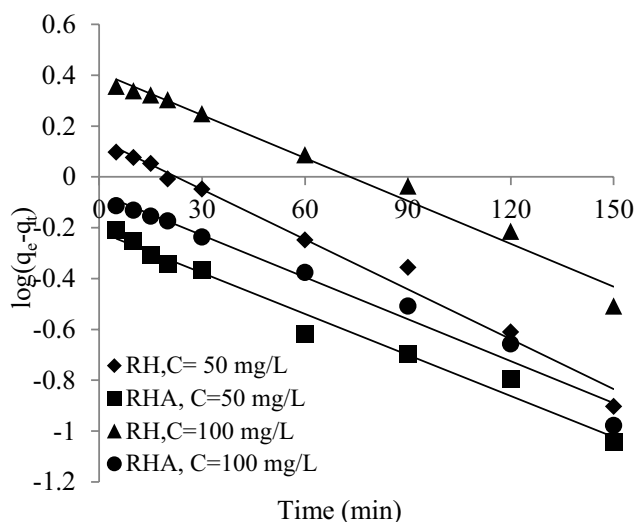


Fig. 6. Pseudo-first-order kinetic plot for adsorption of Cr(VI) onto RH and RHA (conditions: $C_0 = 50$ and 100 mg/L; pH 2; $m = 20$ g/L, $t = 150$ min, stirring speed = 200 rpm, $T = 298$ K).

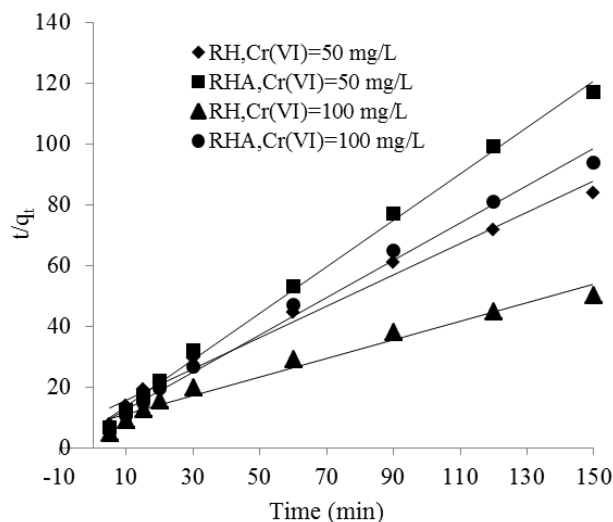


Fig. 7. Pseudo-second-order kinetic plots for adsorption of Cr(VI) onto RH and RHA (conditions: $C_0 = 50$ and 100 mg/L; pH 2; $m = 20$ g/L, $t = 150$ min, stirring speed = 200 rpm, $T = 298$ K).

Table 3

Kinetics parameters for adsorption of Cr(VI) on RH and RHA at different initial Cr(VI) concentration

Adsorbent	Initial Cr(VI) concentration (mg/L)	$q_{e,exp}$ (mg/g)	Pseudo-first-order			Pseudo-second-order			Intraparticle model			
			q_e (mg/g)	K_1 (min^{-1})	R^2	q_e (g/mg/min)	K_2 (min^{-1})	R^2	H (g/mg/min)	K_w (mg/g $\text{min}^{0.5}$)	R^2	C (mg/g)
RH	5	0.41	0.471	0.020	0.970	0.269	0.155	0.997	0.011	0.012	0.988	0.097
	50	1.92	1.158	0.015	0.986	1.950	0.025	0.985	0.094	0.117	0.994	0.383
	100	3.29	1.509	0.013	0.982	3.280	0.012	0.972	0.126	0.204	0.994	0.452
RHA	5	0.42	0.671	0.028	0.948	0.461	0.098	0.997	0.021	0.018	0.984	0.181
	50	1.37	0.805	0.012	0.980	1.310	0.096	0.997	0.165	0.052	0.977	0.664
	100	1.70	0.938	0.013	0.977	1.630	0.060	0.992	0.160	0.068	0.996	0.748

of intraparticle diffusion was explored by using Weber and Morris's model with varying adsorbate concentrations. As shown in Table 3 and Fig. 8, the experimental data were fitted to the intraparticle diffusion model. However, the regression lines did not pass through the origin of the plot, and a positive intercept (Fig. 8) was observed at each concentration, indicating many other processes were also involved in adsorption, all of which may be operating simultaneously. Considering the concentration of adsorbate in solution, mass transfer of ions from boundary layer to adsorbate was not likely limiting the rate of adsorption. The rate constant (K_w) for intraparticle diffusion model (Table 3) increased with an increase in Cr(VI) concentration, which validated the observed reduction in the pseudo-second-order constant and the increase in the rate of adsorption as a function of ion concentration. Further, deviations of straight line from the origin (intercept) indicate that the pore diffusion is not the sole rate-controlling process and the value of the intercept C increases with increasing Cr(VI) concentration (Table 3), indicating that chemisorptions effects are more significant at higher ion concentration.

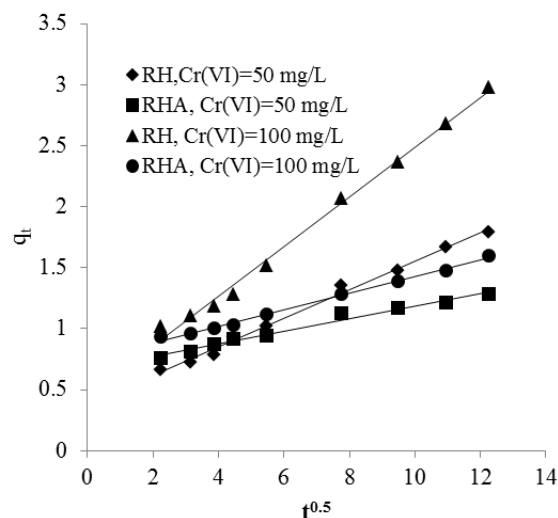


Fig. 8. Intraparticle diffusion model plot of Cr(VI) adsorption on RH and RHA.

3.6. FTIR, SEM, and EDS analysis

The study so far indicates that both RH and RHA can adsorb Cr(VI) from aqueous solution. An effort was made to identify the functional groups present on the surface of the adsorbents, as well as the changes in vibrational frequency of functional groups, by examining FTIR spectra. The FTIR spectra of RH and RHA, fresh and Cr(VI)-loaded, are shown in Figs. 9 and 10, and demonstrate the presence of various functional groups on the surface of RH and RHA. As seen in Fig. 9(a), the prominent peaks at 3,431.2, 2,932.8, 1,747, and 1,097.4 cm^{-1} can be assigned to the stretching vibration of –OH, C–H, C=O, and C–O and Si–O groups, respectively

[32]. The additional peak at 920 cm^{-1} can be assigned to the aromatic out-of-plane ring bends. However, in case of Cr(VI)-loaded RH (Fig. 9(b)), there were significant changes in positions and shapes of peaks between 3,200–2,700, 1,850–1,650, and 1,100–950 cm^{-1} , which correspond to C–H, C=O, and C–O and Si–O groups, indicating Cr(VI) binding mostly with C–H, C=O, and C–O and Si–O groups. Similarly, RHA showed strong peaks at 2,920.9, 1,747, and 1,079.6 cm^{-1} (C–H, C=O, and C–O and Si–O groups, respectively) (Fig. 10(a)), and shifted to 2,930.8, 1,733.1, and 1,077.5 cm^{-1} , respectively, after binding with Cr(VI) (Fig. 10(b)). These characteristics indicate that –OH, C–H, and C=O, C–O and Si–O groups are effective in the adsorption of Cr(VI) onto RH or RHA. The

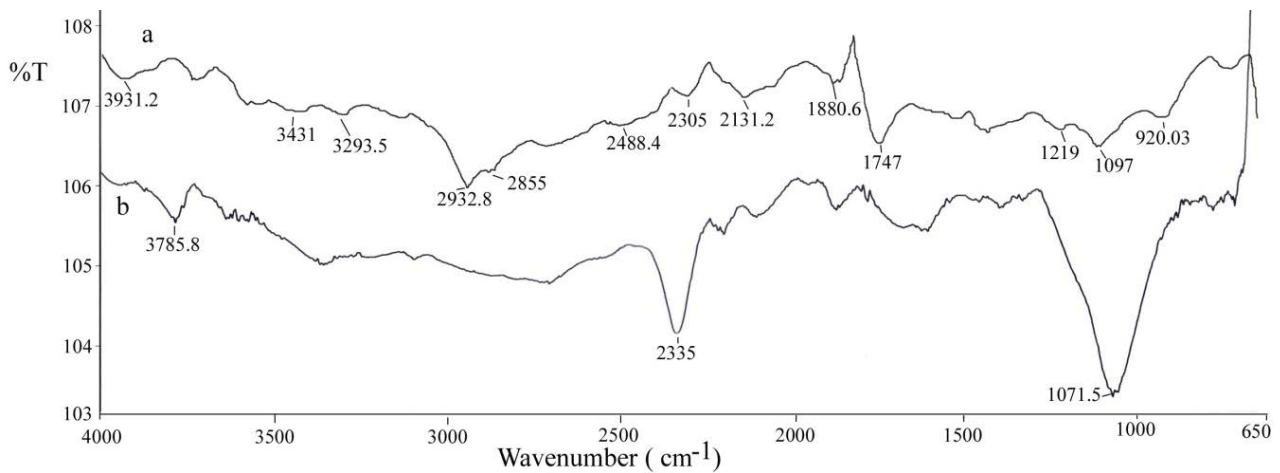


Fig. 9. FTIR analysis of (a) fresh and (b) Cr(VI)-loaded RH.

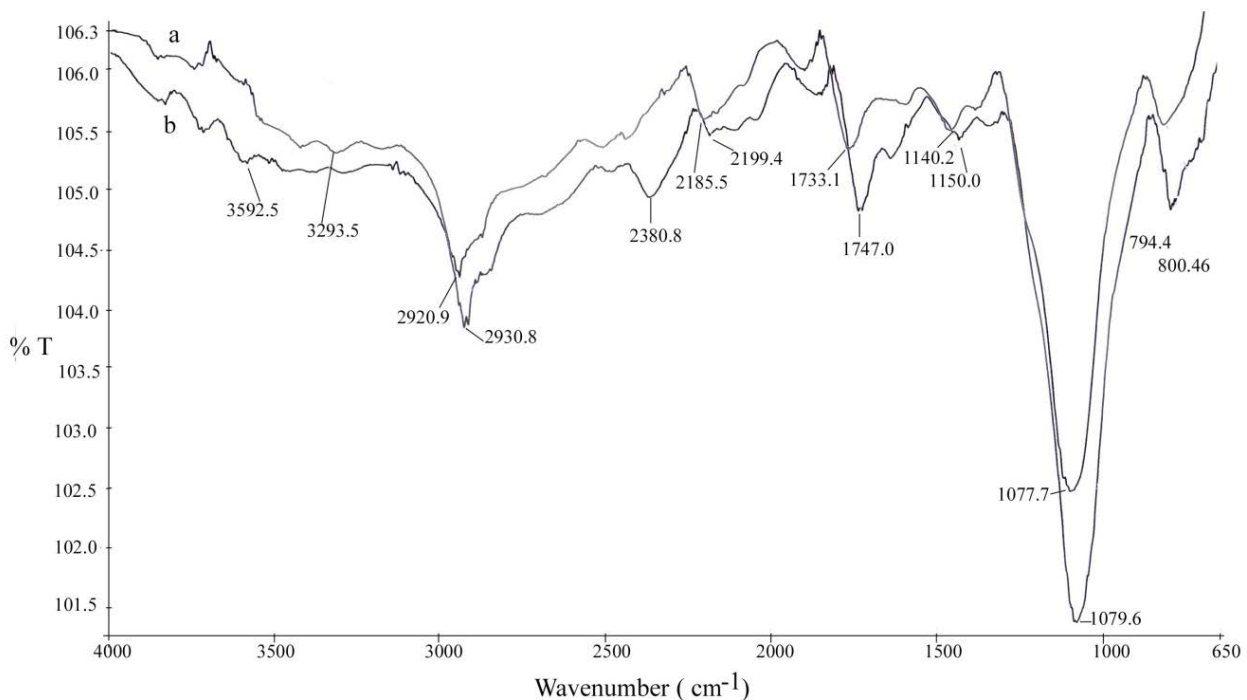


Fig. 10. FTIR analysis of (a) fresh and (b) Cr(VI)-loaded RHA.

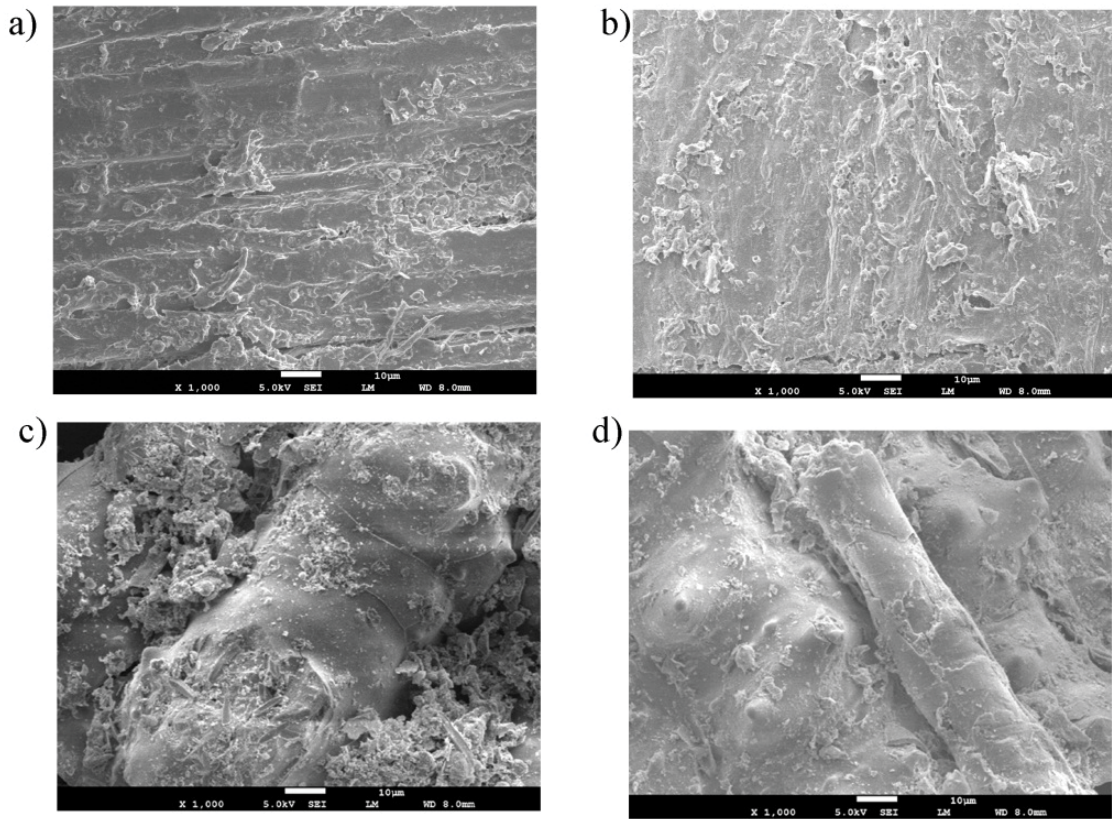


Fig. 11. SEM of (a) fresh RH, (b) Cr(VI)-loaded RH, (c) fresh RHA, and (d) Cr(VI)-loaded RHA.

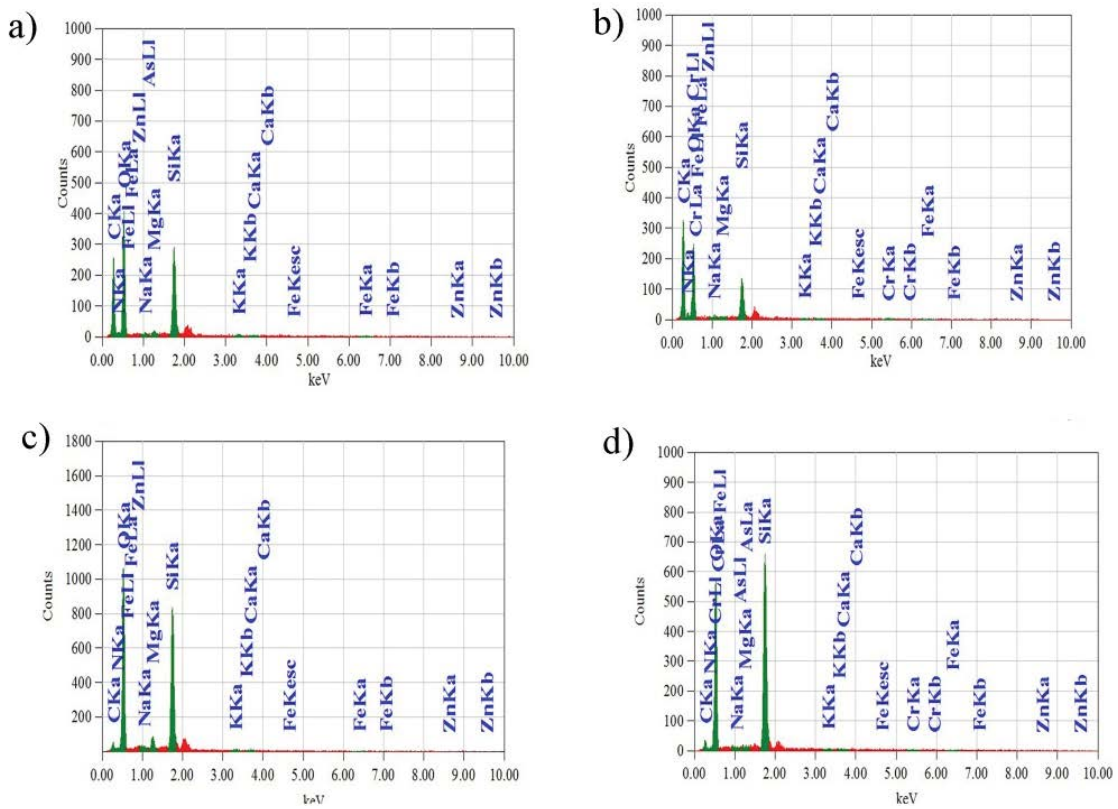


Fig. 12. EDS of (a) fresh RH, (b) Cr(VI)-loaded RH, (c) fresh RHA, and (d) Cr(VI)-loaded RHA.

predominant group involved in the adsorption of metal ions depends on the pH of the solution, which affects the surface chemistry of the adsorbents [21]. At pH 2, the adsorbents surface might be highly protonated which favor the uptake of HCrO_4^- . Therefore, Cr(VI) is likely adsorbed onto RH and RHA through electrostatic attraction and/or by the binding of HCrO_4^- to acidic functional groups on the surface [33]. Thus, the reduction in bands at around 3,400 and 2,900 cm^{-1} indicates the electrostatic interaction between protons of symmetric and asymmetric C–H and –OH functional groups on the surface of RH and RHA with anionic chromium in solution.

Scanning electron microscopy (SEM) along with EDS has been used as a tool for the sorbents characterization (Figs. 11 and 12). The surface of RH and RHA are irregular before Cr(VI) adsorption, but has become shiny due to the deposition of chromium ions after adsorption. The surfaces of fresh adsorbents contained elements of C, N, O, Si, K, and Fe (Figs. 12(a) and (b)). After adsorption, additional signals of chromium are noted in EDS of Cr(VI)-loaded RH and RHA indicating the binding of chromium ions on the RH and RHA (Figs. 12(c) and (d)).

3.7. Removal of Cr(VI) from tannery wastewater by RH and RHA

After completion of basic adsorption experiments, the efficiency of RH and RHA in the removal of Cr(VI) from tannery wastewater was evaluated. Wastewater sample was collected from Hazaribagh Tannery Area, Dhaka, Bangladesh. The pH, EC, TDS, salinity, and Cr(VI) concentration of collected wastewater was determined at the beginning of adsorption experiments, where values of 2.25, 37.2 ms/cm , 24.3 mg/L , 22.7 g/L , and 44.8 mg/L , respectively, were recorded. The pH of the wastewater and the optimal pH obtained from basic adsorption experiments were identical; thus, chemical adjustment of the pH was unnecessary. Batch adsorption studies were carried out at the room temperature, 200 rpm for various contact time (5–180 min). The RH and RHA dose were 20 g/L . Fig. 13 illustrates Cr(VI) removal from tannery wastewater. As shown in Fig. 13, the removal of Cr(VI) increased with time and reached 85.49% for RH and 79.88% for RHA. Thus, RH and RHA are applicable as effective adsorbent for the removal of Cr(VI) from industrial wastewater.

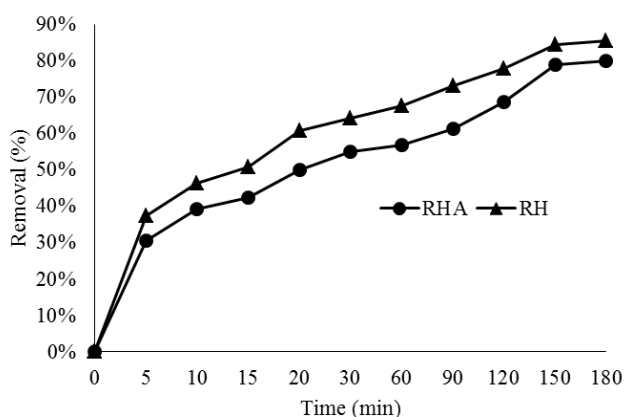


Fig. 13. Removal of Cr(VI) from tannery wastewater by RH and RHA.

4. Conclusion

The study was undertaken to test the ability of RH and RHA for the adsorptive removal of Cr(VI) from aqueous solution. The adsorption process has been shown to be affected from experimental conditions, such as pH, adsorbent dosage, contact time, and initial Cr(VI) concentration. Maximum Cr(VI) removal was observed at pH 2. The efficiencies of RH and RHA for Cr(VI) removal were 94.0% and 88.4%, respectively, from solutions containing 5.0 mg/L of Cr(VI) at adsorbent dose of 20 g/L . The Langmuir isotherm had a better fit with the experimental data with maximum adsorption capacity of 3.78 and 2.27 mg/g for RH and RHA, respectively. Furthermore, RH and RHA removed Cr(VI) from tannery wastewater. Thus, RH and RHA are efficient adsorbents for industrial application.

The kinetics of adsorption of Cr(VI) was best described by pseudo-second-order reaction. The results revealed that the rate of adsorption was controlled by chemisorption and intraparticle diffusion. The FTIR analysis confirms the complexation of Cr(VI) with functional groups present in the adsorbents. Due to availability, low- or no-cost, adsorption capacity and favorable kinetics, RH and RHA hold high promise for practical application of adsorptive removal of Cr(VI) from industries effluent in developing countries like Bangladesh and should be investigated for its practical application.

Acknowledgments

We thank KURITA water and environment foundation for financial support through KWEF research grant (17P037) for this study. The authors would like to extend thanks to The World Academy of Science (TWAS) for instrumental facility under the COMSTECH-TWAS Joint Research Grants Programme (TWAS Ref: 13-371 RG/ENG/AS_C; UNISCO FR: 3240279207).

References

- [1] A. Zhitkovich, Importance of chromium-DNA adducts in mutagenicity and toxicity of chromium (VI), *Chem. Res. Toxicol.*, 18 (2005) 3–11.
- [2] X.S. Wang, L.F. Chen, F.Y. Li, K.L. Chen, W.Y. Wan, Y.J. Tang, Removal of Cr (VI) with wheat residue derived black carbon: reaction mechanism and adsorption performance, *J. Hazard. Mater.*, 175 (2010) 816–822.
- [3] D. Mohan, C. Pittman, Activated carbons and low cost adsorbents for remediation of tri- and hexavalent chromium from water, *J. Hazard. Mater. B*, 137 (2006) 762–811.
- [4] K.K. Krishnani, S. Ayyappan, Heavy metals remediation of water using plants and lignocellulosic agrowastes, *Rev. Environ. Contam. Toxicol.*, 188 (2006) 59–84.
- [5] V.K. Gupta, K.T. Park, S. Sharma, D. Mohan, Removal of chromium(VI) from electroplating industry wastewater using bagasse fly ash – a sugar industry waste material, *Environmentalist*, 19 (1999) 129–136.
- [6] X. Zhou, T. Korenaga, T. Takahashi, T. Moriwake, S. Shinoda, A process monitoring/controlling system for the treatment of wastewater containing chromium (VI), *Water Res.*, 27 (1993) 1049–1054.
- [7] N. Kongsricharoern, C. Polprasert, Chromium removal by a bipolar electrochemical precipitation process, *Water Sci. Technol.*, 34 (1996) 109–116.
- [8] D. Petruzzelli, R. Passino, G. Tiravanti, Ion exchange process for chromium removal and recovery from tannery wastes, *Ind. Eng. Chem. Res.*, 34 (1995) 2612–2617.

- [9] H.F. Shaalan, M.H. Sorour, S.R. Tewfik, Simulation and optimization of a membrane system for chromium recovery from tanning wastes, *Desalination*, 141 (2001) 315–324.
- [10] C.A. Kozłowski, W. Walkowiak, Removal of chromium (VI) from aqueous solutions by polymer inclusion membranes, *Water Res.*, 36 (2002) 4870–4876.
- [11] J.J. Testa, M.A. Grela, M.I. Litter, Heterogeneous photocatalytic reduction of chromium (III) over TiO₂ particles in the presence of oxalate: involvement of Cr(VI) species, *Environ. Sci. Technol.*, 38 (2004) 1589–1594.
- [12] L. Khezami, R. Capart, Removal of chromium(VI) from aqueous solution by activated carbons: Kinetic and equilibrium studies, *J. Hazard. Mater.*, 123 (2005) 223–231.
- [13] V.K. Gupta, A. Rastogi, Biosorption of hexavalent chromium by raw and acid-treated green alga *Oedogonium hatei* from aqueous solutions, *J. Hazard. Mater.*, 163 (2009) 396–402.
- [14] T. Srinath, T. Verma, P.W. Ramteke, S.K. Garg, Chromium (VI) biosorption and bioaccumulation by chromate resistant bacteria, *Chemosphere*, 48 (2002) 427–435.
- [15] M. Samuel, E.A. Abigali, R. Chidambaram, Isotherm modelling, kinetic study and optimization of batch parameters using response surface methodology for effective removal of Cr(VI) using fungal biomass, *PLoS One*, 10 (2015) e0116884, doi:10.1371/journal.pone.0116884.
- [16] V. Sarin, K.K. Pant, Removal of chromium from industrial waste by using eucalyptus bark, *Bioresour. Technol.*, 97 (2006) 15–20.
- [17] M. Aoyama, M. Kishino, T.-S. Jo, Biosorption of Cr (VI) on Japanese Cedar Bark, *Sep. Sci. Technol.*, 39 (2005) 1149–1162.
- [18] H. Gao, Y. Liu, G. Zeng, W. Xu, T. Li, W. Xia, Characterization of Cr(VI) removal from aqueous solutions by a surplus agricultural waste-rice straw, *J. Hazard. Mater.*, 150 (2008) 446–452.
- [19] The International Rice Research Institute Philippines, Available at: <http://irri.org/rice-today/a-second-life-for-rice-husk>, Accessed 16.04.2016.
- [20] K.K. Krishnani, X. Meng, C. Christodoulatos, V.M. Boddu, Biosorption mechanism of nine different heavy metals onto biomatrix from rice husk, *J. Hazard. Mater.*, 153 (2008) 1222–1234.
- [21] M. Bansal, U. Garg, D. Singh, V.K. Garg, Removal of Cr(VI) from aqueous solutions using pre-consumer processing agricultural waste: a case study of rice husk, *J. Hazard. Mater.*, 162 (2009) 312–320.
- [22] K.M.S. Sumathi, S. Mahimairaja, R. Naidu, Use of low-cost biological waste sand vermiculite for removal of chromium from tannery effluent, *Bioresour. Technol.*, 96 (2005) 309–316.
- [23] V.C. Srivastava, I.D. Mall, I.M. Mishra, Characterization of mesoporous rice husk ash (RHA) and adsorption kinetics of metal ions from aqueous solution onto RHA, *J. Hazard. Mater. B.*, 134 (2006) 257–267.
- [24] W.S.W. Ngah, A. Musa, Adsorption of humic acid onto chitin and chitosan, *J. Appl. Polym. Sci.*, 69 (1998) 2305–2310.
- [25] S. Lagergren, Zurtheorie der sogenannten adsorption gelosterstoffe, *Kungliga Svenska Vetenskapsakademiens, Handlingar*, 24 (1898) 1–39.
- [26] Y.S. Ho, G. McKay, The kinetic of sorption of divalent metal ion onto sphagnum moss peat, *Water Res.*, 34 (2000) 735–742.
- [27] W.J. Weber, J.C. Morris, Kinetics of adsorption on carbon from solution, *J. Sanitary Eng. Div. ASCE*, 89 (1963) 13–59.
- [28] X.S. Wang, L.F. Chen, F.Y. Li, K.L. Chen, W.Y. Wan, Y.J. Tang, Removal of Cr (VI) with wheat-residue derived black carbon: reaction mechanism and adsorption performance, *J. Hazard. Mater.*, 175 (2010) 816–822.
- [29] K. Kadirvelu, C. Namasivayam, Activated carbon from coconut coir pit as metal adsorbent: adsorption of Cd (II) from aqueous solution, *Adv. Environ. Res.*, 7 (2003) 471–478.
- [30] M. Jain, V.K. Garg, K. Kadirvelu, Equilibrium and kinetic studies for sequestration of Cr(VI) from simulated wastewater using sunflower waste biomass, *J. Hazard. Mater.*, 171 (2010) 328–334.
- [31] O.S. Bello, O.M. Adelaide, M.A. Hamed, O.A.M. Popoola, Kinetic and equilibrium studies of methylene blue removal from aqueous solution by adsorption on treated sawdust, *Maced. J. Chem. Chem. Eng.*, 29 (2010) 77–85.
- [32] W. Nakbanpote, P. Thiraveetyan, C. Kalambaheti, Preconcentration of gold by rice husk ash, *Miner. Eng.*, 13 (2000) 391–400.
- [33] L. Levankumar, V. Muthukumar, M.B. Gobinath, Batch adsorption and kinetics of chromium (VI) removal from aqueous solutions by *Ocimum americanum* L. seed pods, *J. Hazard. Mater.*, 161 (2009) 709–713.